Ellipsometry-based study of poled glass refractive index depth profiles

I. Fabijanić, P. Pervan, B. Okorn, J. Sancho-Parramon, V. Janicki*

Ruđer Bošković Institute, Bijenička c. 43, 10000 Zagreb, Croatia
**janicki@irb.hr*

Abstract: Application of electric field and moderately elevated temperature is depleting the side facing anode from alkali present in glasses. The change of composition of the treated glass results in variation of refractive index depth profile within the treated glass. Spectroscopic ellipsometry is employed for characterization of optical properties of glass treated in different conditions. The results of optical characterization are verified by secondary ion mass spectroscopy. It is found that the refractive index profile obtained from ellipsometry has maximum value higher than the one of untreated glass. Obtained refractive index profiles are in very good agreement with concentration profiles.

1. Introduction

Soda-lime glasses contain alkali species, like Na_2O, CaO, MgO, K_2O, Al_2O_3, which in total can reach nearly 30% of its composition. At moderately elevated temperatures and under the influence of electric field imposed by placing the glass slide between electrodes, the alkali ions drift towards the cathode. As a consequence, the glass slide side placed beneath the anode becomes depleted of alkali ions that are, depending on their mobility, pushed deeper into the bulk and even diffuse out at the cathode side [1]. Depletion of positive ions at one side and their accumulation at some depth are inducing a formation of an internal electric field. This field has permanent character, unless the sample is heated above the glass transition temperature [2]. The process of forming the internal electric field inside glass due to ion drift is called glass poling. Depletion induces structural changes in glass. The region that was placed beneath the anode presents lower refractive index [3-5]. For these properties poled glass is used for waveguides [6], imprinting diffractive gratings on its surface [7-10] and also for etching since material from the poled region is more easily removed [11-13]. Recently, poled glass has been proposed as a substrate for micro structuring thin metal layers [14].

If glass surface is coated with thin metal layer, or metal nanoparticles are embedded into the glass matrix, electric field assisted dissolution (EFAD) of metal is taking place simultaneously with poling. Electric field is stripping electrons from metal and metal ions are drifting into the glass to fill the vacancies left after alkali ions drift deeper into matrix. In this way EFAD is used for glass doping with different metals [15-18].

A common technique involved to study depth profile of the poled glass composition is secondary ion mass spectrometry (SIMS). SIMS has confirmed diffusion of Na, Ca, Mg, Mn and K towards cathode, while Al concentration does not change [2, 16, 17, 19-21]. Due to their different mobility and formation of internal electric field, Ca and K concentrations form peaks, with Ca maxima closer to the anode treated surface. Na concentration does not form a peak, but is smoothly rising to the value corresponding to the untreated glass, situated deeper in the glass.

Characterization of poled glass refractive index (n) and its depth profile ($n(d)$) is not so standard as SIMS studies, although it is important for application of such glass. For example, the change of refractive index of the glass after EFAD is a result of its decrease due to depletion and increase due to metal ion doping. In this case it is important to distinguish the metal ions contribution to the change of optical properties from the contribution of glass poling. For this purpose, poled glass $n(d)$ should be determined first. The poled glass $n(d)$ were obtained from interferometry [3], by the use of leaky modes [22] and micro-IR reflectometry [3], for example. These studies agree that the refractive index of depleted region is approaching to the one of fused silica and towards bulk is is approaching to that of untreated glass. Also, the width of the depleted region and its refractive index depends on the poling conditions. Ellipsometry is one of the noninvasive techniques enabling optical characterization of materials, but it is seldom used for poled glass [5]. The aim of this work is to study $n(d)$ of the samples obtained under different poling conditions, using spectroscopic ellipsometry data as a basis for numerical modeling of optical constants and to estimate in such way how reliable and useful these results may be.

2. Experimental

In this study, poling was applied to microscopy glass slides, 1 mm thick (VWR Microscope Slides) consisting of 73.7% SiO_2, 12.6% Na_2O, 7.0% CaO, 4.1% MgO, 1.5% Al_2O_3 and 0.6% K_2O. This is a typical composition of soda lime glass. Chromium coated glass plate was used as an anode, providing a smooth contact with the microscopy slide surface. An Al plate was used as a cathode. The glass slide was placed between the electrodes and put into a furnace. This setup was heated 1 hour before the voltage application. The samples were pre-heated to prevent increase of temperature during poling thus preventing an increase of alkali ions mobility. After the desired poling time, voltage was switched off and the sample cooled naturally. The poling conditions were heating to the temperature 200-300 ^oC with applied potential 350-700 V for 0.5-2 h.

Ellipsometric functions $\Psi(E)$ and $\Delta(E)$ were measured by J. A. Woollam V-VASE ellipsometer in the range 0.61-3.63 eV (corresponding to 342-2033 nm) at 45^o, 55^o and 65^o angles of incidence. WVASE software was used for numerical modeling. Since it is expected that poling modifies the region beneath the surface only, while the interior of the sample remains unaffected, the samples were modeled by a refractive index gradient layer at the top of the substrate having optical properties of untreated glass. The care was taken to keep the number of parameters as low as possible, starting from the model with a single layer having homogeneous refractive index and replacing it with a simple gradient layer if this would improve the quality of the fit significantly. Simple gradient layer has two more parameters than the one with homogeneous refractive index: percent of refractive index variation and the order (exponent) of the gradient shape function. The next step would be introducing a new layer in front or behind the previous one and repeating the procedure.

Additional measurements were performed in order to verify the results. Three samples treated for 2 h at 300^oC (corresponding ellipsometric functions presented in Fig.1.) were chosen for analysis by SIMS. SIMS in-depth profiles were measured by Hiden SIMS Workstation, using 3 keV O^{2+} primary ion beams at the impact angle of 45^o and collecting positive secondary ions. The depth scale of SIMS craters was determined by Dektak XT stylus surface profiler, based on the usual assumption of constant etching rate. Since glass is not conductive, it was necessary to neutralize samples during the measurements in order to avoid charging. For this purpose, an electron gun was bombarding the samples with electrons of 500 eV.

3. Results

The measured ellipsometric functions $\Psi(E)$ and $\Delta(E)$ for the samples treated for 2 h at 300 °C with potentials 350 V, 500 V and 700 V, together with the data obtained from fitting of model optical properties, are presented in Fig.1. The refractive index profiles at 2.48 eV (500 nm) obtained from ellipsometry measurements are in Fig.2-4. Each Figure presents profiles of all the samples obtained by changing just one parameter during poling: Fig.2. the change of potential, Fig.3. the change of temperature and Fig.4. the change of time. Each graph of every Figure is showing profiles of the samples treated under two conditions kept equal and the third one changed. In this way it is possible to follow the evolution of refractive index profile with EFAD conditions. Concentration profiles of different compounds, obtained from SIMS data of the chosen samples (Fig.1., Fig.2.c)) are presented on Fig.5. The concentrations are obtained from the known bulk values of the compounds, that were reached in the regions corresponding to pristine glass where their measured signal recovered to the constant values, and using assumption that number of Si counts should be constant as Si is not drifting during poling. The depth values on *x*-axis are obtained from profilometry measurements of the crater formed by the etching beam. The refractive index profiles of the corresponding samples are plotted in this Figure to make comparison of profiles easier.

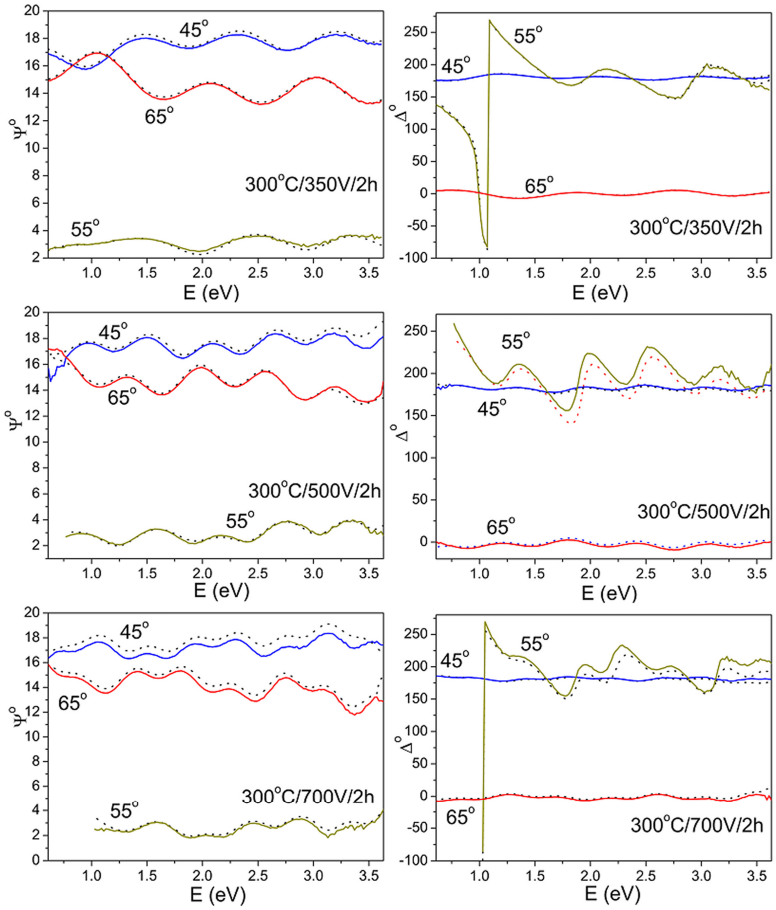

Fig.1. Comparison of the experimental data and the data obtained from optical characterization based on ellipsometry for the samples poled at 300 ºC for 2 h at 350 V, 500 V and 700 V. Ellipsometric functions *Ψ(E)* (upper row) and *Δ(E)* (lower row): experimental (full line) and fitted data (dots).

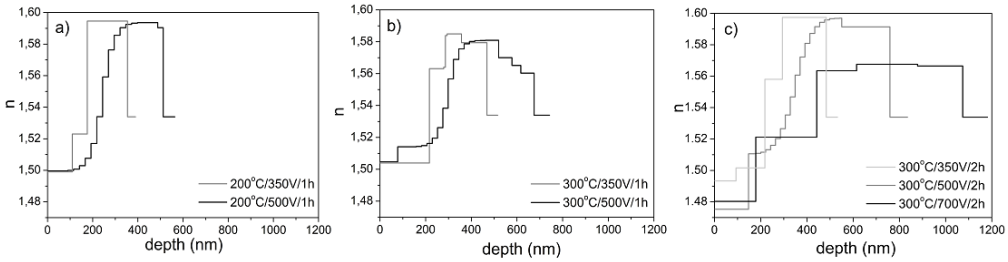

Fig.2. The change of refractive index profile with the potential applied during poling (350 V, 500 V and 700 V). Refractive index profiles are obtained from optical characterization based on ellipsometric measurements of the poled samples. Sample/air interface that was facing anode during poling is at 0 nm. All the profiles end with the refractive index of untreated glass.

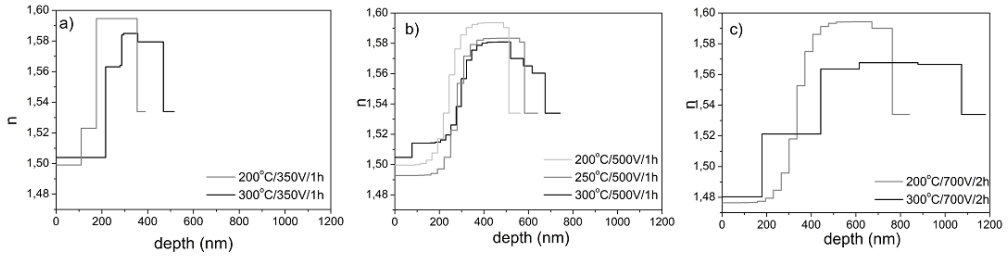

Fig.3. The change of refractive index profile with the poling temperature (200 ºC, 250 ºC and 300ºC) . Refractive index profiles are obtained from optical characterization based on ellipsometric measurements of the poled samples. Sample/air interface that was facing anode during poling is at 0 nm. All the profiles end with the refractive index of untreated glass.

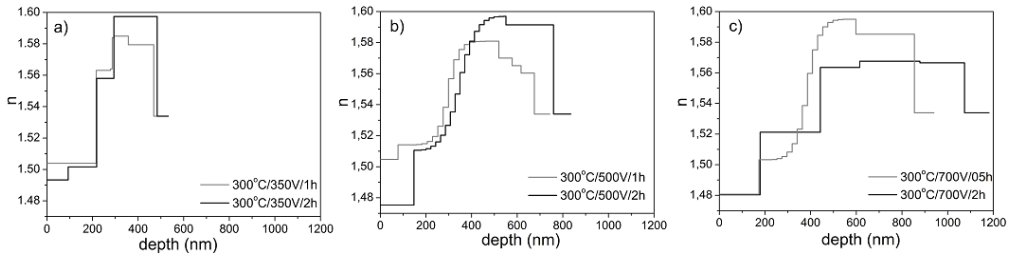

Fig.4. The change of refractive index profile with the time of poling (0.5 h, 1 h and 2 h). Refractive index profiles are obtained from optical characterization based on ellipsometric measurements of the poled samples. Sample/air interface that was facing anode during poling is at 0 nm. All the profiles end with the refractive index of untreated glass.

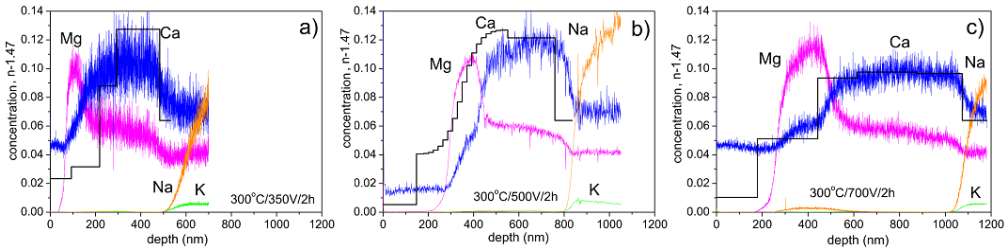

Fig.5. Concentration profiles obtained from SIMS analysis of the same samples as presented in Fig.1 and Fig.2.c) (samples poled at 300 ^{o}C for 2 h with 350 V (a), 500 V (b) and 700 V (c)). For comparison, also the refractive index profiles (reduced by 1.47 to fit into the scale) of the corresponding samples are plotted (black full line).

4. Discussion and conclusions

From ellipsometric functions in Fig.1. it is possible to see the increase of fringes density with the applied poling potential. This indicates appearance of a thin film with refractive index distinct from the one of pristine glass and whose thickness grows with the applied potential. It is in accordance with the model where low refractive index layer next to the air is representing the region of glass that was facing anode and that is penetrating deeper into the glass as the external electric field grows.

It should be noticed that the quality of the data fitting is very good. The fits of the other samples are about the same quality or even better than those presented in Fig.1. Taking into account also that the new parameters in the course of optical characterization were introduced gradually and only in the case they would significantly improve the fit quality, it is reasonable to expect that the obtained refractive index profiles are rather reliable. All the profiles (Fig.2-4.) start with a layer representing the depleted region next to the glass surface. It is followed by the rise of refractive index that reaches maximum and then drops to the pristine glass refractive index value. The appearance of the *n(d)* peak suggests pile up of the alkali species in the interior between the depleted and unaffected region. The refractive index of the first layer is around 1.5, and only for the samples treated at 700 V and the one treated at 300 ^{o}C, 500 V, 2 h, is decreasing to around 1.48. None of the profiles start with refractive index as low as 1.46, that is expected for pure silica. Higher refractive index in this region may be related not only to the possibility that smooth *n(d)* of the sample is too roughly approximated by the model, but also to the possibility that this region is not completely depleted. Also, the surface of the poled glass increased roughness and the depleted region change of structure [23] may be the reasons for a higher refractive index of this region and compensated by increasing refractive index in the first layer of the model.

The appearance of the *n(d)* peak deserves to be discussed in more details. Similar peak in *n(d)* was found after poling of BK7 glass and attributing it with a pile-up K^{+} ions [2]. There, the peak is approximately 0.002 higher than the refractive index of the untreated sample. In the other work of the same author [22] the peak in soda-lime glass of the similar composition as here, poled with 261^{o}C, 400 V, 5h, was not observed. However, the peak reported here is significantly exceeding the refractive index of an untreated microscope slide. For the samples treated in conditions 200-300 ^{o}C, 350-500 V, 0.5-2 h for as much as 0.06-0.07. Only for the sample treated at 300^{o}C, 700 V, 2 h the peak is somewhat lower than the peaks of the other treated samples, approximately 1.57. In Fig.2-4. is possible to notice that the peaks are decreasing with the increase of voltage above 350 V (Fig.2.) or temperature above 200 ^{o}C (Fig.3.). Only at 300 ^{o}C, 350 V and 500 V the peak is still increasing with elapse of time (Fig.4.). This means that the weaker conditions than the applied here are favorable for generation of refractive index maximum in the depth profile of glass. The stronger conditions lead to its flattening, broadening and shifting towards bulk that should be related to the diffusion of ions with low mobility deeper into the bulk. This might be the reason why the *n(d)* peak was not observed in [22].

SIMS depth profile analysis of the samples treated at 300 ^{o}C, 2h with 350 V, 500 V and 700 V (Fig. 5.) presents that next to the surface the concentration of Na, which ions have the

highest mobility in glass, is very close to zero (the level of noise). It sharply increases deeper in the glass. Mg, Ca and K intensities follow the same trend close to the surface. Only the level of Ca in the depleted region is not close to zero. K is following Na and reaches a constant level corresponding to the untreated glass concentration. Ca and Mg pass a maximum before the decrease to a constant value. This corresponds to the drift of the lower mobility ions (Ca, Mg) and an increase of their concentration in the pile up region, observed by other authors as well [1, 2, 6, 7, 19]. Mg has a wide shoulder towards bulk possibly indicating two kinds of Mg species having different mobility.

Overlap of *n(d)* and concentration profiles in Fig.5. a-c) is very good. Of course, one has to keep in mind that the absolute values of one and the other profile cannot be taken into relationship straightforwardly because the relation between concentration of the components and effective refractive index requires application of effective medium theories [24]. Positions and widths of *n(d)* and concentration maxima of Ca are in very good accordance. It should be noticed also that the depth of the refractive index maximum drop corresponds to the depth of the steep Na intensity increase. This supports the assumption that the increase of refractive index above the value of an untreated glass is related with accumulation of some of the alkali species [22] and in the case of soda-lime glass it is in fact Ca. The thickness of the first layer and the width of the depleted region (before Ca or Mg increase), same as the slope of the refractive index and concentration increase are in rougher agreement. In the case that Mg species are not contributing to optical constants so much as those of Ca or Na, the model representing the sample might be too rough to take it into account. On the other hand, if the significance of Mg species is almost like the one of Ca, the obtained profiles maybe have already been taken it into account by properties of the second layer from air (Fig.5.a) and c)) or by the gradient layer that for this reason may be shifted towards the glass surface (Fig.5.b)).

As mentioned before, none of the *n(d)* start with refractive index as low as 1.46, which is expected for pure silica. The hypothesis that the region close to air is not depleted enough may be supported by Ca concentration obtained from SIMS that is not close to zero, like for the other alkalis. However, the other possibilities mentioned above cannot be disregarded.

The stronger poling conditions lead to flattening, broadening and shifting concentration peak deeper towards the bulk that is the behaviour noticed also for refractive index maximum. So, indeed it confirms that this behaviour may be related to the diffusion of low mobility Ca deeper into the bulk.

In brief, although refractive index profiles are not necessarily able to reveal all the details of the refractive index profile that could be expected based on SIMS data, it is shown that models obtained from ellipsometry are capable to reveal the changes in poled glass refractive index satisfactory. Ellipsometry is shown to be a sensitive and effective non-invasive technique appropriate for poled glass refractive index profiling, assuming that the number of free parameters of the model is increased gradually and is well justified. In the case of soda-lime glass, pile up of Ca is responsible for an increase of refractive index above the value of untreated glass in Na depleted region. Mg might also be important and should be taken into account. If the poling conditions are stronger, the accumulation of lower mobility ions is reducing, broadening and shifting towards bulk and the refractive index peak may disappear. These findings will be helpful for the future studies of glass poling in the sense of choosing a proper technique for *n(d)* characterization and the choice of proper poling conditions whether *n(d)* maximum and alkali ions accumulation is desired or not.

Acknowledgements

This work was co-financed by the Croatian Agency for SMEs, Innovations and Investments (HAMAG-BICRO) from the Program for Proof of Innovative Concept (grant no. PoC6_11_45 U-1) and Croatian Science Foundation under the project no. IP-2016-06-2168. Portions of this work were presented at the Optical Interference Coatings (OIC) 2019. (paper ID: 3192974).

5. References

1. E. C. Ziemath, V. D. Araujo and C.A. Escanhoela, Jr., "Compositional and structural changes at the anodic surface of thermally poled soda-lime float glass", J. Appl. Phys. **104** 054912 (2008).
2. A.V. Redkov, V.G. Melehin, D.V. Raskhodchikov, I.V. reshetov, D.K. taganatsev, V.V. Zhurikhina and A.A. Lipovski, "Modifications of poled silicate glass under heat treatment", J.Non-Cryst. Solids **503-504**, 279-283 (2019).
3. R. Oven, "Measurement of planar refractive index profiles with rapid variations in glass using interferometry and total variation regularized differentiation", J. Mod. Opt. **62**, S53-S60 (2015).
4. M. Dussauze, E.I. Kamitsos, E. Fargin, and V. Rodriguez, "Refractive index distribution in the non-linear optical layer of thermally poled oxide glasses", Chem. Phys. Lett. **470**, 63-66 (2009).
5. J. Luo, H. He, N.J. Podraza, L. Qian, C.G. Pantano, and S.H. Kim, "Thermal poling of soda-lime silica Glass with nonblocking electrodes - Part 1: effects of sodium ion migration and water ingress on glass surface structure", J. Am. Ceram. Soc. **99** 1221-1260 (2016).
6. A.L.R. Brennand and J.S. Wilkinson, "Planar waveguides in multicomponent glasses fabricated by field-driven differential drift of cations", Opt. Lett. **27**, 906-908 (2002).
7. L. A. H. Fleming, D. M. Goldie and A. Abdolvand, "Imprinting of glass", Opt. Matter. Express **5**, 1674-1681 (2015).
8. L.A.H. Fleming, S. Wackerow, A.C. Hourd, W.A. Gillespie, G. Seifert and A. Abdolvand, "Diffractive optical element embedded in silver-doped nanocomposite glass" Opt. Express **20** 22579 -22584 (2012).
9. A. Lipovskii, V. Zhurikhina and D. Taganatsev, "2D-structuring of glass via thermal poling: a short review", Int. J. Appl. Glass Sci. **9** 24-28 (2018)
10. G. Yang, M. Dussauze, V. Rodriguez, F. Adamietz, N. Marquestaut, K.L.N. Deepak, D. Grojo, O. Uteza, P. Delaporte, T. Cardinal, and E. Fargin, "Large scaled micro-structured optical second harmonic generation response imprinted on glass surface by thermal poling", J. Appl. Phys. **118** 043105 (2015).
11. S.E. Alexandrov, A.A. Lipovskii, A.A. Osipov, I.V. Reduto and D.K. Taganatsev, "Plasma-etching of 2D-poled glasses: A route to dry litography", Appl. Phys Lett. **111** 111604 (2017).
12. Reduto, A. Kamenskii, A. redkov, A. Lipovskii, "Mechanisms and peculiarities of electric field imprinting in glasses", J. Electrochem. Soc. **164** E385-E390 (2017).
13. Reduto, A. Kamenskii, P. Brunkov, V. Zhurikhina, Y. Svirko and A. Lipovskii, "Relief micro- and nanostructures by the reactive ion and chemical etching of poled glasses", Opt. Mater. Express **9** 3059-3068 (2019).
14. V. Janicki, I. Fabijanić, B. Okorn, P. Dubček, and J. Sancho-Parramon, " Selective electric field assisted dissolution as a technique for micro and nano structuring of metal thin films", Appl. Phys. Lett. **113**, 183508 (2018).
15. F. Mezzapesa, I.C.S. Carvalho, P. Kazansky, O. Deparis, M. Kawazu, K. Sakaguchi, "Bleaching of sol-gel glass film with embedded gold nanoparticles by thermal poling" Appl. Phys. Lett. **89** 183121 (2006).
16. F. Gonella, P. Canton, E. Cattaruzza, A. Quaranta, C. Sada and A. Vomiero, "Field-assisted ion diffusion of transition metals for the synthesis of nanocomposite silica glass" Mater. Sci. Eng. C **26** 1087-1091 (2006).
17. E. Cattaruzza, F. Gonella, S. Ali, C. Sada and A. Quaranta, "Silver and gold doping of SiO_2 glass by solid-state field-assisted dissolution", J. Non-Cryst. Solids, **355** 1136-1139 (2009).
18. N. Takamure, A. Kondyurin and D.R. McKenzie, "Electric field assisted ion exchange of silver in soda-lime glass: a study of ion depletion layers and interactions with potassium", J. Appl. Phys. **125** 175104 (2019).
19. R.G. Gossink, "SIMS analysis of a field-assisted glass-to-metal seal" J. Am. Cer. Soc. **61** 539-540 (1978).
20. T.G. Alley and S.R.J. Brueck, "Secondary ion mass spectrometry study of space-charge formation in thermally poled fused silica", J. Appl. Phys. **86** 6634-6640 (1999).
21. S. Ali, Y. Iqbal, M. Ajmal, F. Gonella, E. Cattaruzza and A. Quaranta, "Field-driven diffusion of transition metal and rare-earth ions in silicate glasses" J. Non-Cryst. Solids **405** 39-44 (2014).
22. R. Oven, "Measurement of the refractive index of electrically poled soda-lime glass using leaky modes", Appl. Opt. **55**, 9123-9130 (2016).
23. A.N. Miliou, R.Srivastava, and R.V. Ramaswamy, "Modelling of the index change in K^+-Na^+ ion-exchanged glass", Appl. Opt. **30** 674-681 (1991).
24. V. Janicki, J. Sancho-Parramon, H. Zorc, "Refractive index profile modelling of dielectric inhomogeneous coatings using effective medium theories", Thin Solid Films **516** 3368-3373 (2008).